Neuro-Oncology Advance Access published November 30, 2010
Neuro-Oncology
doi:10.1093/neuonc/noq143
NEURO-ONCOLOGY

Assessment of perfusion MRI-derived parameters in evaluating and predicting response to antiangiogenic therapy in patients with newly diagnosed glioblastoma

Emma Essock-Burns, Janine M. Lupo, Soonmee Cha, Mei-Yin Polley, Nicholas A. Butowski, Susan M. Chang, and Sarah J. Nelson

Department of Radiology and Biomedical Imaging (E.E-B., J.M.L., S.C., S.J.N.), UCSF/UCB Joint Graduate Group in Bioengineering (E.E-B., S.J.N.), Department of Bioengineering and Therapeutic Sciences (S.J.N.), Department of Neurological Surgery (S.C., M-Y.P., N.A.B., S.M.C.), University of California–San Francisco

The paradigm for treating patients with glioblastoma multiforme (GBM) is shifting from a purely cytotoxic approach to one that incorporates antiangiogenic agents. These are thought to normalize the tumor vasculature and have shown improved disease management in patients with recurrent disease. How this vascular remodeling evolves during the full course of therapy for patients with newly diagnosed GBM and how it relates to radiographic response and outcome remain unclear. In this study, we examined 35 patients who were newly diagnosed with GBM using dynamic susceptibility contrast (DSC) MRI in order to identify early predictors of radiographic response to antiangiogenic therapy and to evaluate changes in perfusion parameters that may be predictive of progression. After surgical resection, patients received enzastaurin and temozolomide, both concurrent with and adjuvant to radiotherapy. Perfusion parameters, peak height (PH) and percent recovery, were calculated from the dynamic curves to assess vascular density and leakage. Six-month radiographic responders showed a significant improvement in percent recovery between baseline and 2 months into therapy, whereas 6-month radiographic nonresponders showed significantly increased PH between baseline and 1 month. At 2 months into therapy, percent recovery was predictive of progression-free survival. Four months prior to progression, there was a significant increase in the standard deviation of percent recovery within the tumor region. DSC perfusion imaging provides valuable information about vascular remodeling during antiangiogenic therapy, which may aid clinicians in identifying patients who will respond at the pretherapy scan and as an early indicator of response to antiangiogenic therapy.

Keywords: antiangiogenic therapy, DSC, enzastaurin, GBM, MRI, perfusion imaging.

Glioblastoma multiforme (GBM) is the most malignant subtype of glioma and is characterized by extreme heterogeneity, extensive neovasculature, and active angiogenesis. The current standard of care for patients with newly diagnosed GBM includes combined radio- and chemotherapy, which comprises a 6-week cycle of external beam radiation therapy and oral temozolomide followed by an additional 6 months of temozolomide.[1,2] Antiangiogenic therapies have recently shown the potential for reducing tumor size and increasing 6-month progression-free survival (PFS).[3,4] The recent phase II trial of the antiangiogenic agent bevacizumab, a monoclonal antibody directed against vascular endothelial growth factor (VEGF), used alone and in combination with irinotecan reported dramatic improvement in 6-month PFS and a high response rate in patients with recurrent GBM.[5] It has been proposed that the use of adjuvant antiangiogenic therapy in combination with standard radio- and chemotherapy acts to normalize the tortuous tumor vasculature and improve delivery of chemotherapeutics and

Received June 2, 2010; accepted August 13, 2010.

Correspondence Author: Emma Essock-Burns, BS, Department of Radiology and Biomedical Imaging, University of California–San Francisco, UCSF Mail Code 2532, Byers Hall Room #303, 1700 4th Street, San Francisco, CA 94158-0223 (emma.essock-burns@radiology.ucsf.edu).

oxygen.[6,7] Enzastaurin (LY317615) is one such antiangiogenic agent that is currently under investigation for its potential as an adjuvant therapy for patients with newly diagnosed GBM.[8]

Enzastaurin selectively inhibits protein kinase Cβ and has been reported to have both direct antitumor effects, through suppression of tumor cell proliferation and induced apoptosis, and indirect effects, through inhibition of tumor-induced angiogenesis.[9] Unlike bevacizumab, enzastaurin is a non-VEGF antiangiogenic agent whose mechanism of action is not yet fully understood.[10] Preclinical reports have shown that enzastaurin and radiation are synergistic in combination to induce apoptosis in glioma models.[11] One of the first multicenter phase II clinical studies of enzastaurin was reported by Robertson et al.,[12] who described a favorable toxicity profile and a single-agent activity in a population of 55 patients with refractory diffuse large B-cell lymphoma. The authors highlight the possibility of differential sensitivity to enzastaurin based on a small subset of the study population who showed a long-term response but showed steady-state drug levels similar to those of the rest of the population. In the recurrent GBM population, enzastaurin has not been shown to have superior efficacy compared with the cytotoxic chemotherapeutic agent lomustine,[13] yet there are several ongoing phase I/II trials that involve the use of adjuvant enzastaurin for patients newly diagnosed with GBM.[8,14]

The exciting potential of adjuvant antiangiogenic therapy for improving disease management and increasing PFS has simultaneously highlighted unresolved questions in the field regarding the evaluation of response. As described in van den Bent et al.,[15] there are numerous challenges in evaluating response to antiangiogenic therapies in neuro-oncology. Classic Macdonald criteria[16] have used a reduction in contrast-enhancing volume as a surrogate marker for antitumor effects. For antiangiogenic therapies, the apparent reduction in enhancing volume could be due to the transient normalization of the blood–brain barrier rather than the antitumor activity.[17,18] This complicates the definition of progression and the use of 6-month PFS as a surrogate endpoint of overall survival. As the paradigm for GBM therapy shifts from a purely cytotoxic approach to now incorporating targeted therapies with cytostatic effects, there is a need to explore the use of functional imaging techniques in order to better evaluate and define new criteria for evaluating response to therapy.

A number of noninvasive imaging techniques have been used to assess changes in microvasculature and response to therapy.[19–21] Dynamic susceptibility contrast (DSC) magnetic resonance imaging (MRI) has been shown to improve sensitivity compared with conventional MRI alone in determining the glioma grade.[22] Within the context of antiangiogenic therapy, Batchelor et al.[3] used both DSC and dynamic contrast-enhanced (DCE) MRI, with a variety of other advanced imaging techniques, to evaluate the normalization of vasculature in recurrent GBM patients receiving adjuvant AZD2171 during the first 112 days of therapy. The authors observed a rapid functional vascular normalization in terms of both a reduction in vessel size and overall permeability, which was found to be reversible upon drug "holiday." The changes in DSC and DCE imaging–derived perfusion parameters combined with differences in circulating collagen IV levels between pretherapy and 1-day post-therapy were combined to create a "vascular normalization index" that was predictive of overall survival (OS) and PFS for patients with recurrent GBM who received this therapy.[23] How these parameters evolve during the full course of therapy for patients with newly diagnosed GBM and how they relate to radiographic response and outcome remain unknown.

The previous work with DSC perfusion MRI has made it an alluring technique for evaluating response to antiangiogenic therapy. There is the potential for addressing challenges specific to assessing the efficacy of antiangiogenic agents in clinical trials, including (i) the identification of subpopulations that would benefit most from this therapy and (ii) the recognition of early markers of progressive disease in the case of tumor recurrence.[17] The present study was designed to investigate the use of DSC perfusion MRI to identify early predictors of overall response to antiangiogenic therapy as well as to evaluate distinct changes in MR parameters during therapy that may be predictive of imminent progression.

Materials and Methods

Patient population

Thirty-five patients who were newly diagnosed with grade IV GBM based on the WHO criteria were recruited for this study. Patients received surgical resection and were treated with a standard 6-week cycle of external beam radiation therapy. In addition to radiotherapy, patients were also administered a chemotherapy regimen that included temozolomide (75 mg/m^2 daily during radiotherapy and 200 mg/m^2 for 5 days every 28-day cycle after radiotherapy) and enzastaurin (250 mg daily) concurrent with and adjuvant to radiation therapy. Patient age ranged from 25 to 70 years, with a median age of 57 years. Patients were required to have a Karnofsky performance score (KPS) of $\geq$60 in order to be enrolled in the study. Patients who went off therapy due to side effects were excluded from the study population. All patients provided informed consent in accordance with guidelines established by the Committee on Human Research at our institution.

Imaging

MR exams were performed on a 3T GE EXCITE scanner (GE Healthcare Technologies) with an eight-channel phased array receive coil. Patients were imaged prior to beginning therapy (postsurgical resection) and then serially at 1, 2, 4, 6, 8, 10, and 12

Table 1. Pattern of therapy and number of DSC patient scans acquired at each time-point

	Time (mos)								
	Baseline	**1**	**2**	**4**	**6**	**8**	**10**	**12**	**Total**
Therapy	RT + Drug	RT + Drug	RT + Drug	Drug	Drug	Drug	Drug	Drug	145
DSC scans	29	19	28	22	17	14	11	5	

RT indicates external beam radiation therapy (60 Gy, 5 days per week for 6 weeks).
"Drug" includes enzastaurin (250 mg daily) and temozolomide (75 mg/m^2 daily during RT; 200 mg/m^2 for 5 days every 28 days after RT).

months after beginning therapy. If a patient progressed, his or her subsequent scans were no longer included in this study.

Conventional MRI and MR spectroscopy imaging—The MRI examination included pre- and postgadolinium T1-weighted 3-dimensional spoiled gradient echo (SPGR) with inversion recovery (repetition time [TR] = 8.86 milliseconds, echo time [TE] = 2.50 milliseconds, matrix = 256 × 256, slice thickness = 1.5 millimeters, field of view [FOV] = 24 × 24 centimeters, inversion time [TI] = 400 milliseconds, flip angle = 15°) and T2-weighted fluid attenuated inversion recovery (FLAIR) (TR = 150 milliseconds, TE = 2.1 milliseconds, TI = 2.38 seconds, matrix = 256 × 192, slice thickness = 3 millimeters, FOV = 24 × 24 centimeters) imaging. Patients also received lactate-edited 3D MR spectroscopy (MRS) with point-resolved spectroscopy sequence localization and very selective saturation pulses around an excited volume of ~80 × 80 × 40 mm^3 (TR = 1104 milliseconds, TE = 144 milliseconds, FOV = 16 × 16 × 16 centimeters, nominal voxel size = 1 × 1 × 1 centimeters, 712 dwell points, 988 Hz sweepwidth).[24] After each examination, the images were transferred to a SUN Ultra 10 workstation (Sun Microsystems) for postprocessing. The pregadolinium SPGR, FLAIR, and MRS images were aligned to the postgadolinium SPGR images for each scan date.[25]

Perfusion-weighted imaging—In addition to anatomic and metabolic imaging, patients received DSC imaging, as summarized in Table 1. Perfusion imaging was performed during the injection of gadolinium chelate contrast (Magnevist, Bayer Healthcare). A bolus injection of 0.1 mmol/kg contrast agent was administered at 3 mL/s using a power injector. A gradient-echo echo-planar sequence (TR = 1500 milliseconds, TE = 54 milliseconds, matrix = 128 × 128, FOV = 24 × 24 cm^2, slice thickness = 4 millimeters, flip angle = 35°) was acquired for 2:00 minutes for a total of 80 time-points.

Image processing

The T2* signal-intensity time curves acquired during the first pass of the gadolinium bolus were converted to change in the relaxation rate (ΔR2*) and resampled to match the spatial resolution of the anatomic image series. Two parameters were derived from these curves: *peak height* (PH), the maximum increase in relaxivity reflective of the greatest gadolinium influx and a physiologic estimate of vascular density; and *percent recovery*, the relative return to baseline of the curve reflective of the bolus passed through the voxel and a physiologic estimate of leakage. A schematic representation of these parameters on the susceptibility curve is illustrated in Fig. 1. These summary parameters were chosen in lieu of relative cerebral blood volume and leakage factor, which can also be derived from the susceptibility curve, as they have been shown to be proportional to each other for the data acquisition parameters used in this study but do not require extensive curve fitting.[26] DSC images were nonrigidly aligned to the precontrast SPGR image using a B-spline warping by maximization of normalized mutual information.[27] The PH value was normalized to the mean value within the normal-appearing white matter, which was segmented from the precontrast SPGR images by applying a hidden Markov random field model with an expectation–maximization algorithm.[28]

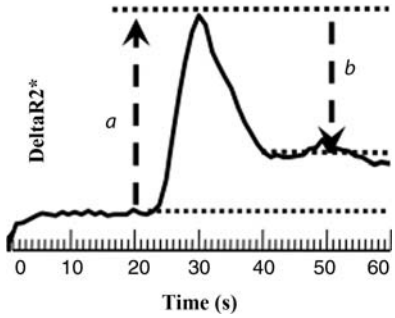

Fig. 1. Summary parameters of susceptibility curve. PH, equal to the distance *a*, is the maximum increase in relaxivity and is a physiologic estimate of vascular density. Percent recovery, equal to [the distance *b*/the distance *a*] × 100, is the relative return to the baseline of the susceptibility curve and is a physiologic estimate of leakage.

Definition of putative tumor region

The region of risk was identified using both anatomic and metabolic imaging (Fig. 2). The contrast-enhancing lesion (CEL) was defined on the postgadolinium T1-weighted image, and the T2 hyperintense region (T2All) was defined on the T2 FLAIR image using a semiautomatic segmentation algorithm[29] (Fig. 2A,

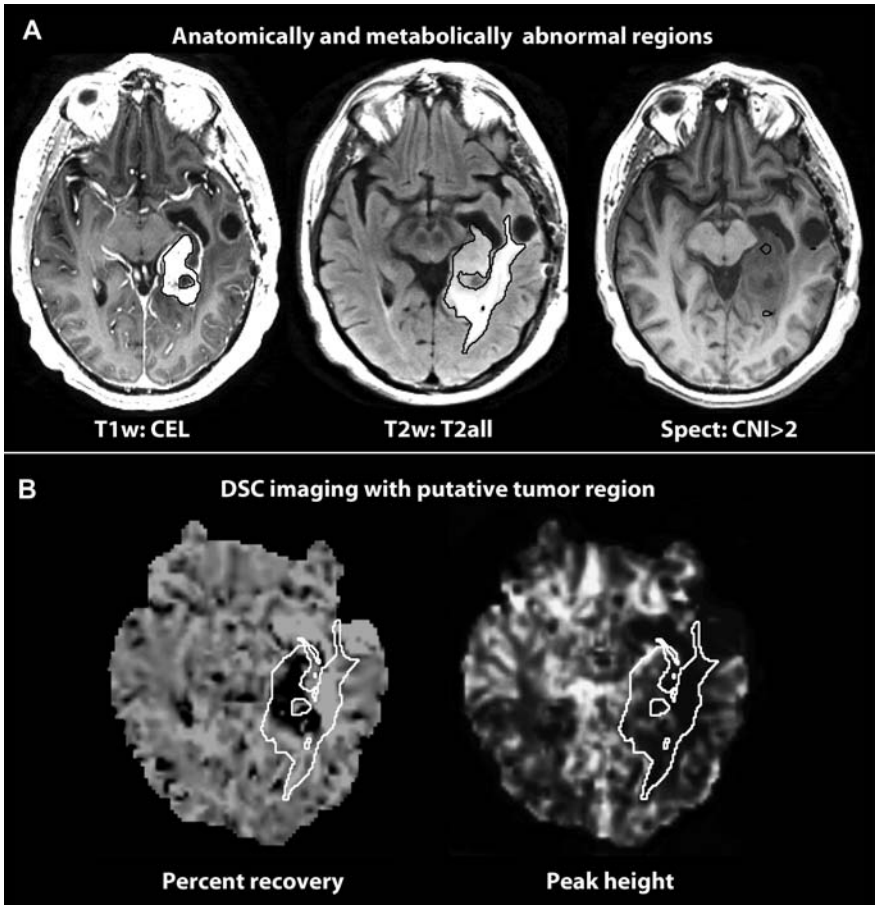

Fig. 2. Definition of putative tumor region. (A) Anatomically and metabolically abnormal regions were combined to define the putative tumor region, which was overlaid on both the percent recovery and PH parametric maps (B).

left and middle). A board-certified radiologist approved all regions of interest. The region of abnormally elevated choline-to-*N*-acetylaspartate index (CNI >2)[30] was defined on the MRS image (CNI mask; Fig. 2A, right). The putative tumor region was defined as including these 3 abnormality masks (CEL, T2All, and CNI mask) and excluding the resection cavity, cerebral spinal fluid, and necrotic regions (Fig. 2B).

Data analysis/statistical considerations

The putative tumor region mask was overlaid on the parametric maps derived from the DSC perfusion-weighted imaging techniques (Fig. 2B). Two measures of abnormality were extracted from each of the parametric maps within the putative tumor region: the "intensity" and the "heterogeneity" of the perfusion parameter value. The intensity of the most extreme portion of the abnormality for the vascular density parametric maps was defined as the 90th percentile value of the DSC-derived PH corresponding to elevated vascularization. For the permeability parametric maps, intensity was defined as the 25th percentile DSC-derived percent recovery corresponding to elevated permeability. The perfusion heterogeneity was defined as the standard deviation of the perfusion parameter value within the putative tumor region reflective of the variation in the extent of vascularization or permeability on the respective parametric map. The logrank test was used to compare PFS and OS among response groups. PFS was defined as the time from the patient's baseline scan to the scan date of clinical progression, or in the case of no progression, patients were censored at the date of last contact. To address the potential for pseudoprogression, the clinical histories of all patients who progressed within 12 weeks of the completion of radiotherapy as well as those of all patients with a suspect scan followed by stable disease were centrally re-reviewed by a neuro-oncologist. Notation was made regarding reoperation and location of recurrence to confirm true progression in accordance with the recommendations set forth by Wen et al.[31] The Wilcoxon rank-sum test was used to test for differences in imaging parameters between response groups at early time-points, and the Wilcoxon sign-rank test was used to test for within-group change between early time-points. Univariate and multivariate nonparametric Cox regression analyses were used to evaluate which parameters were predictive of PFS or OS (landmarked from scan date of perfusion covariate). Clinical control factors of baseline KPS, age, gender, and extent of resection (the few cases of biopsy were collapsed

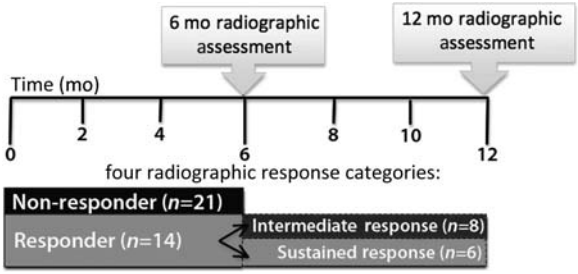

Fig. 3. Radiographic response categories schema. Timeline showing the 2 radiographic response assessments done at 6 and 12 months after the beginning of radiotherapy and a decision-tree flowchart of the 4 radiographic response categories. At the 6-month radiographic assessment, patients were divided into 2 groups. Patients with decreased enhancement were classified as "6-month radiographic responders" ($n = 14$). Patients with increased ($n = 18$) or no change ($n = 3$) in enhancement were classified as "6-month radiographic nonresponders" ($n = 21$). The 6-month radiographic responder patients were further subdivided at the 12-month radiographic assessment in order to capture the durability of the response. Six-month responder patients who showed an obvious resurgence of enhancement by the 12-month radiographic assessment were classified as having a "12-month intermediate response" ($n = 8$), whereas patients who continued to show a decrease or no change in the enhancement were classified as having a "12-month sustained response" ($n = 6$).

with subtotal resection) were included in this analysis. Owing to the exploratory nature of the study, no formal adjustment of type I error was undertaken; in all cases, $P < .05$ was considered statistically significant.

Definition of radiographic response

Patients were divided into 4 radiographic response categories based on the assessment made by an experienced board-certified radiologist at 2 different time-points (6 and 12 months). A flowchart illustrating this decision-tree process is displayed in Fig. 3. The assessments were done blinded to the patients' perfusion data.

Six-month radiographic assessment—The radiologist reviewed the series of anatomic images from each patient up to this time-point to determine the changes in contrast enhancement from the baseline scan. Patients with decreased enhancement were classified as "6-month radiographic responders" ($n = 14$). Patients with increased ($n = 18$) or no change ($n = 3$) in enhancement were classified as "6-month radiographic nonresponders" ($n = 21$). Figure 4A shows a characteristic example of a 6-month radiographic nonresponder (top) and 6-month radiographic responder (middle and bottom). Note the obvious increase in the CEL of the nonresponder and decrease in the CEL of the responders.

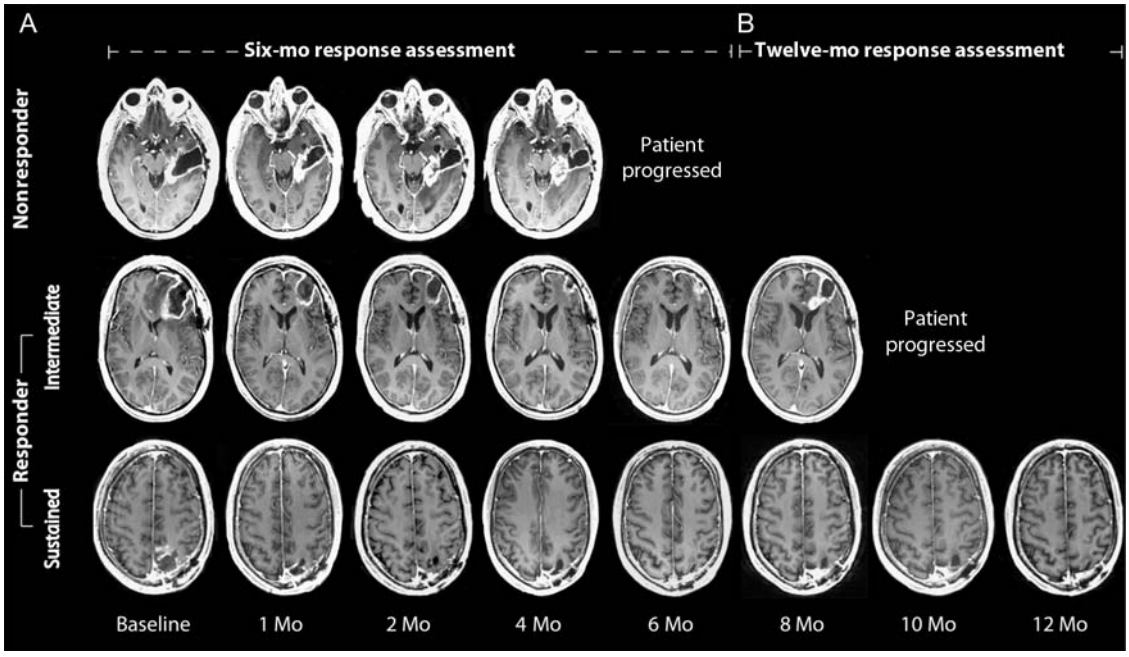

Fig. 4. Radiographic response assessment. T1-weighted postgadolinium serial images of 3 exemplar patients of each of the response categories. Six-month nonresponders (top) had a significant increase in contrast enhancement (CE) within the 6-month assessment (A), while 6-month responders (middle and bottom) did not. Those patients who responded during the 6-month assessment showed 2 distinct patterns of CE upon the further 12-month assessment (B). Patients with a 12-month intermediate response had a dramatic resurgence of CE (middle), whereas those with a 12-month sustained response did not (bottom).

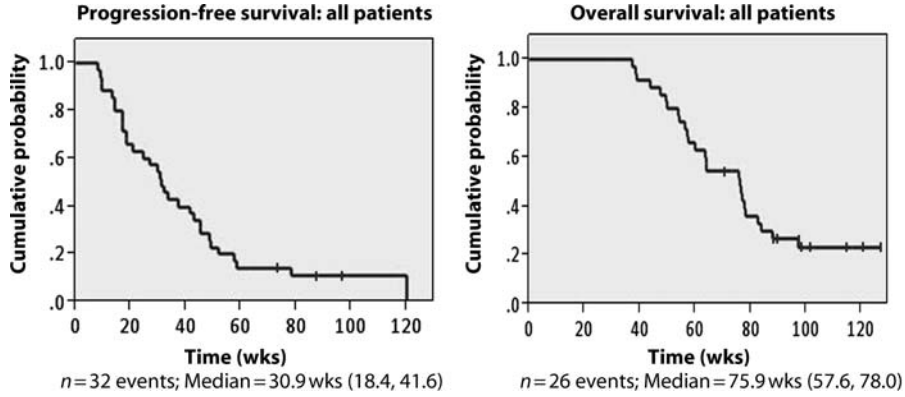

Fig. 5. The Kaplan–Meier analysis. The Kaplan–Meier PFS and OS curves for the 35 GBM patients.

Twelve-month radiographic assessment—In order to capture the durability of the response for the 14 patients who were classified as "6-month radiographic responders," a second assessment was performed 12 months after the beginning of radiation. Patients who showed an obvious resurgence of contrast enhancement were classified as having a "12-month intermediate response" ($n = 8$), and those who continued to show a decrease or no change in the enhancement were classified as having a "12-month sustained response" ($n = 6$). Figure 4B shows examples of 2 of these patients, one where the observed response is transient (middle) and the other where the observed response is sustained (bottom).

This classification allowed the data to be analyzed in terms of patients who showed no short-term radiographic response; those who showed an intermediate radiographic response; and those that showed a sustained radiographic response during the 1 year of follow-up imaging. The rationale for doing both 6- and 12-month assessments is 2-fold. First, it reduces the risk of mistakenly capturing a pseudoprogression event because the radiographic pattern is assessed at 2 discrete standard clinical time-points. Second, by delineating between intermediate and sustained responses, it allows the identification of imaging characteristics associated with patients who benefit the most from therapy.

Results

A total of 145 patient scans were collected with an average of 18 patient scans per time-point (Table 1). The Kaplan–Meier curves describing PFS and preliminary OS of the 35 patients are displayed in Fig. 5. Thirty-two of the 35 patients were determined by their neuro-oncologist to have evidence of progression during the length of the study. All patients who progressed within 12 weeks of the completion of radiotherapy ($n = 13$) were confirmed to have had true progression; 11 patients had histological confirmation at resurgery, 1 patient had new CEL outside of the high-dose radiation field, and 1 patient changed therapies and quickly progressed again. Median PFS for the entire population was 30.9 weeks (95% CI: 18.4–41.6 weeks) and median OS, based on 26 events, was 75.9 weeks (95% CI: 57.6–78.0 weeks). Median follow-up time for the censored patients at study completion was 98.9 weeks.

Early differences in perfusion parameters among radiographic response groups

Data were analyzed from baseline pretherapy scan through progression or furthest follow-up with a particular emphasis on identifying early predictors of response.

PH: measure of vascularization

Normalization of entire population—The greatest change in the 90th percentile PH across the patients occurred within the first 2 months of therapy (Fig. 6B, top). There was a significant within-patient reduction in the 90th percentile PH and the standard deviation of PH in the putative tumor region between baseline and 2 months after initial therapy scans (Wilcoxon sign-rank, $P = .002$; $P = .008$). After 4 months of therapy, there were no longer any significant within-patient changes for either the 90th percentile PH or the standard deviation of PH between sequential bimonthly scans across the population.

Radiographic response assessment—Within the first 2 months of antiangiogenic drug administration, there was a significant reduction in the 90th percentile PH between the 1- (during RT) and 2-month scans (Wilcoxon sign-rank, $P = .008$), but not between the baseline and 1-month scans. However, this lack of significance is explained by distinct differences within the radiographic response groups, as summarized in Table 2.

Figure 6A shows the PH parametric map from a 6-month nonresponder patient, as well as examples of responder patients with either a 12-month intermediate response or sustained response, at baseline and 1 month into therapy. Both the patients with a 12-month

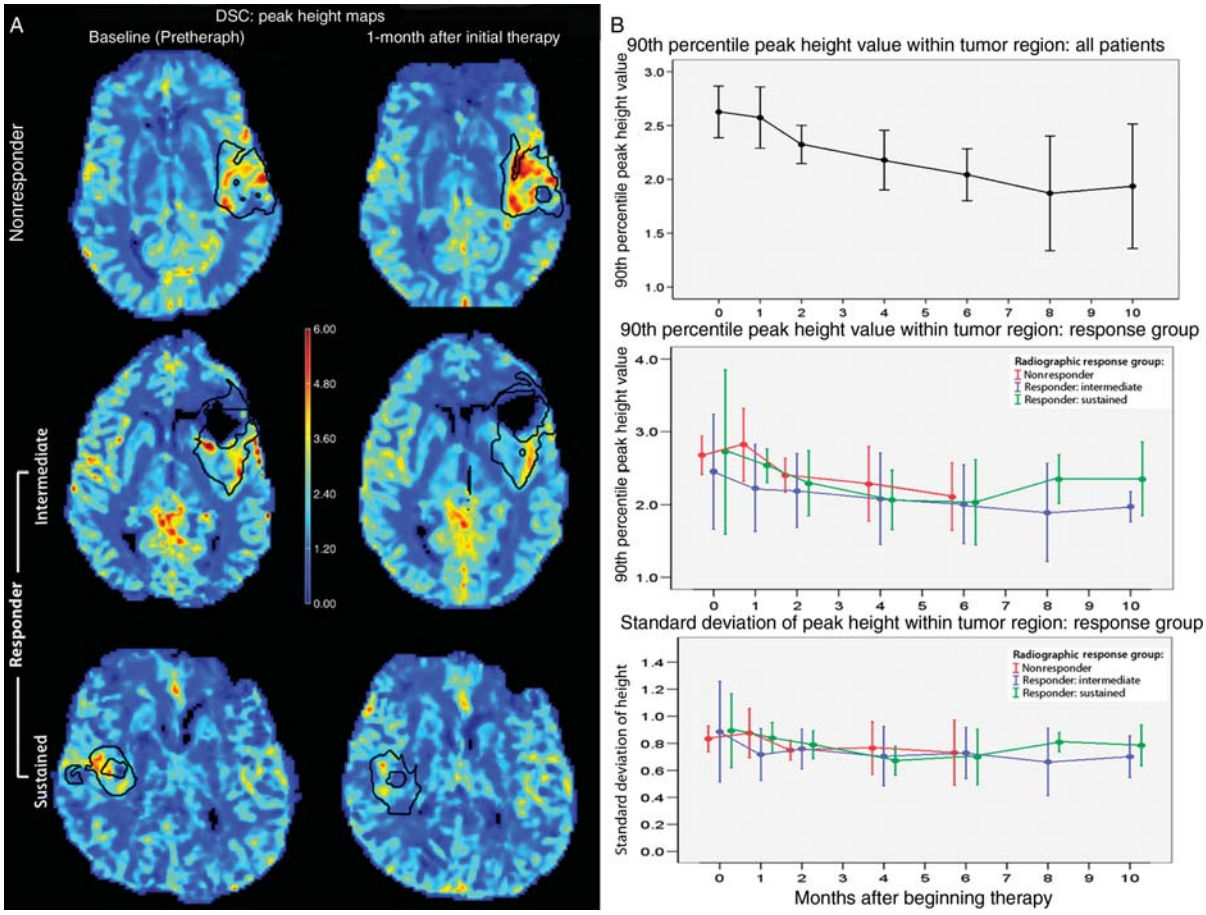

Fig. 6. Peak height. (A) PH parametric maps of patient examples of each response category at baseline and 1 month into therapy. Note the increase in PH of the 6-month nonresponder patient (top) and the decrease in PH of the patient with a 12-month intermediate response (middle) and the patient with a 12-month sustained response (bottom) within the putative tumor region (black line). (B) PH over time for the entire population (top) and by the response group (middle and bottom). Greatest amount of change in 90th percentile PH occurred within the first 2 months of therapy.

intermediate response and the patients with a 12-month sustained response showed a similar mean decrease between the baseline and 1-month scans: -0.19 ± 0.63 and -0.27 ± 0.58, respectively, whereas the 6-month nonresponders showed a mean increase of 0.21 ± 0.57 (Table 2, PH). Although the amount of change was not significantly different between response groups, it did have implications for PFS, which is discussed within the context of progression predictors.

The initial vascularization varied for the various response groups. Six-month nonresponders and the patients with a 12-month sustained response had similar baseline vascularization (90th percentile PHs of 2.68 ± 0.51 and 2.67 ± 0.62), whereas patients with a 12-month intermediate response were initially lower (2.45 ± 0.93; Table 2, PH) and after the first month of therapy were significantly reduced compared with the rest of the population (2.23 ± 0.57; Table 2, PH, Wilcoxon rank-sum, $P < .03$). The reduced 90th percentile PH value can also be seen in the patient example with 12-month intermediate response in Fig. 6A (middle) compared with the 6-month nonresponder (top) and 12-month sustained response patient (bottom) examples.

Percent Recovery: measure of vascular permeability

Normalization of entire population—Unlike PH, the percent recovery parameter was not found to have a specific period during which there were significant within-patient changes for the entire population. Rather, by as early as 2 months after the initial therapy, significant differences had begun to emerge in both the value and heterogeneity of the recovery within the putative tumor region between response groups.

Radiographic response assessment—Figure 7A displays the parametric maps of percent recovery at 2 months after initial therapy for one 6-month nonresponder patient and two 6-month responder patients with either a 12-month intermediate response or sustained response. Significant differences were found at 2

Table 2. Summary of PH and percent recovery data during the first 2 months of therapy and at progression for each response group

	PH									
	Mean intensity (90th percentile value)[a]					Mean heterogeneity (SD)[a]				
	Baseline	1 mo	Δ(Baseline, 1 mo)	2 mos	Progression[b]	Baseline	1 mo	Δ(Baseline, 1 mo)	2 mos	Progression[b]
Nonresponders ($n = 21$)	2.67 ± 0.51	2.82 ± 0.64	0.20 ± 0.53	2.40 ± 0.41	2.29 ± 0.64	0.83 ± 0.19	0.88 ± 0.24	0.06 ± 0.22	0.75 ± 0.13	0.76 ± 0.24
Responders: intermediate ($n = 8$)	2.45 ± 0.93	2.23 ± 0.57	−0.27 ± 0.58	2.19 ± 0.60	2.30 ± 0.56	0.91 ± 0.43	0.72 ± 0.18	−0.22 ± 0.33	0.76 ± 0.18	0.81 ± 0.21
Responders: sustained ($n = 6$)	2.67 ± 0.62	2.53 ± 0.14	−0.19 ± 0.62	2.29 ± 0.36		0.86 ± 0.16	0.84 ± 0.07	−0.05 ± 0.14	0.79 ± 0.08	
All patients ($n = 35$)	2.63 ± 0.62	2.57 ± 0.59	−0.02 ± 0.58	2.32 ± 0.46	2.29 ± 0.60	0.86 ± 0.25	0.82 ± 0.20	−0.04 ± 0.26	0.76 ± 0.13	0.78 ± 0.23
	Percent recovery									
	Mean intensity (25th percentile value)[a]					Mean heterogeneity (SD)[a]				
	Baseline	1 mo	2 mos	Δ(Baseline, 2 mos)	Progression[b]	Baseline	1 mo	2 mos	Δ(Baseline, 2 mos)	Progression[b]
Nonresponders ($n = 21$)	75.0% ± 9.3	76.4% ± 12.4	71.8% ± 18.5	−2.7% ± 12.0	75.9% ± 17.9	9.4% ± 2.6	9.2% ± 3.7	12.7% ± 5.8	3.1% ± 5.1	11.1%v5.7
Responders: intermediate ($n = 8$)	78.8% ± 4.5	81.3% ± 2.2	82.1% ± 4.0	3.9% ± 3.8	77.1% ± 8.3	10.8% ± 3.1	8.7% ± 1.8	10.3% ± 3.3	−0.9% ± 4.1	12.0% ± 4.8
Responders: sustained ($n = 6$)	76.5% ± 5.0	80.6% ± 4.2	83.7% ± 3.5	7.2% ± 7.0		10.8% ± 4.0	9.30% ± 2.8	10.3% ± 3.5	−0.6% ± 6.6	
All patients ($n = 35$)	76.1% ± 7.8	78.8% ± 8.8	76.8% ± 14.7	1.0% ± 10.3	76.2 ± 15.6	10.0% ± 3.0	9.2% ± 2.9	11.6 ± 4.88	1.3% ± 5.3	11.3% ± 5.4

[a]Mean computed across all patients in group.
[b]Includes only patients who had progressed, so was analyzed by 6-month radiographic response group.

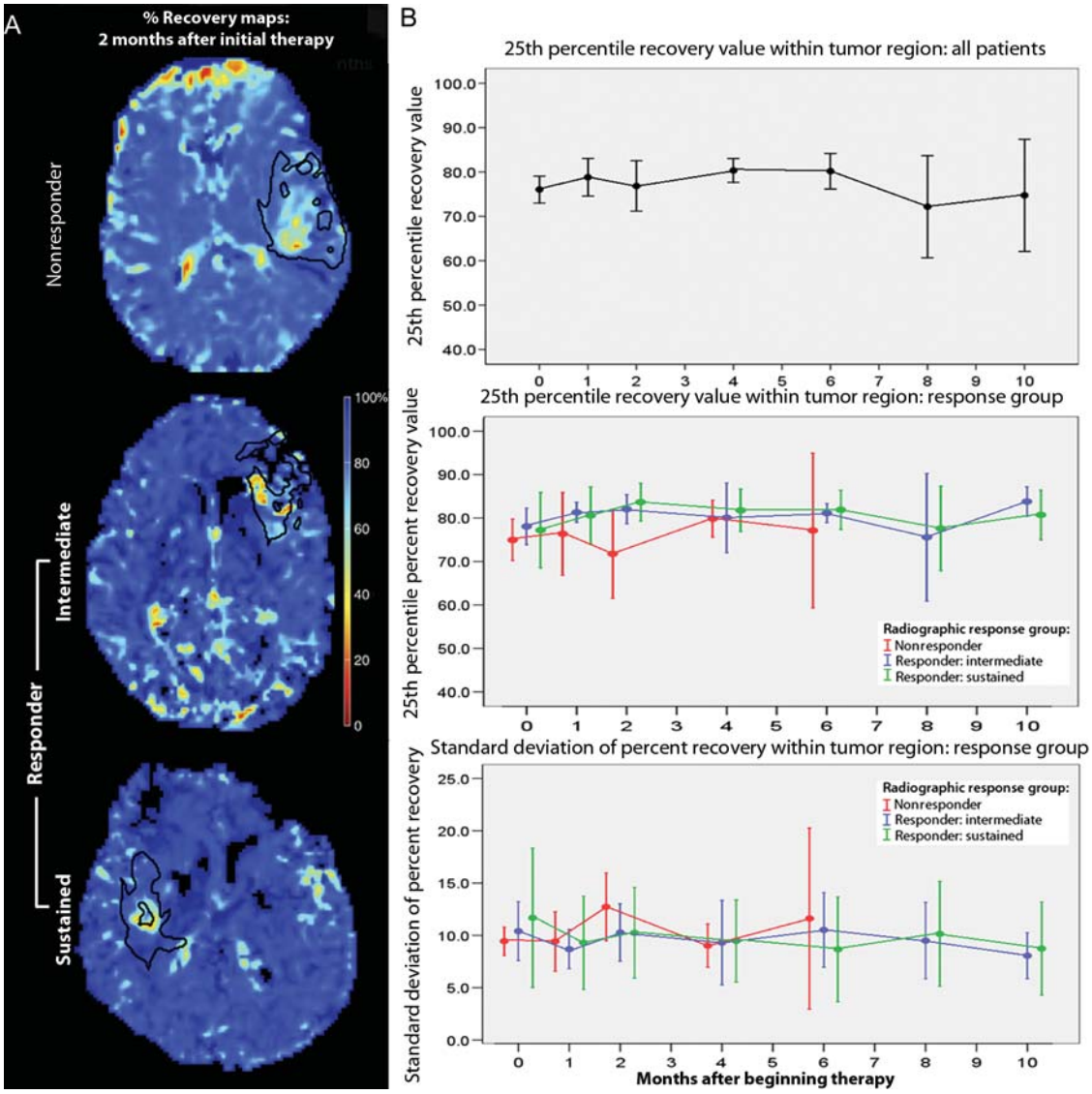

Fig. 7. Percent recovery. (A) Percent recovery parametric maps of patient examples of each radiographic response category at 2 months into therapy. Note the reduced percent recovery of the 6-month nonresponder patient (top) compared with the patient with a 12-month intermediate response (middle) and the patient with a 12-month sustained response (bottom) within the putative tumor region (black line). The 25th percentile value within the putative tumor region was further predictive of PFS at this time-point. (B) Percent recovery over time for the entire population (top) and by the response group (middle and bottom).

months after initial therapy among the 6-month response groups, as described later. Note the reduced recovery and increased heterogeneity throughout the putative tumor for the 6-month nonresponder (top) compared with both of the 6-month responders (middle and bottom).

Six-month nonresponders displayed significantly lower 25th percentile recovery (71.8% ± 18.5%) than 6-month responders (82.7% ± 3.7%) at 2 months into therapy (Wilcoxon rank-sum, $P = .01$). The 6-month responder group showed significant improvement in the 25th percentile recovery value between the baseline and 2-month scan (Wilcoxon sign-rank, $P = .008$), whereas the 6-month nonresponders did not show a significant within-patient change (Wilcoxon sign-rank, $P = .64$). Six-month nonresponders had instead undergone a highly variable decrease in the 25th percentile recovery value (−2.7% ± 12.5%) and a marginally significant increase in overall heterogeneity (3.1 ± 5.3; Wilcoxon sign-rank, $P = .05$) by this time-point. Table 2 (percent recovery) shows the 25th percentile recovery and the standard deviation for each of the radiographic response groups.

Early imaging predictors of progression and survival

The data were analyzed to identify any patterns of perfusion parameters that were predictive of imminent progression and of OS. Of the 35 patients enrolled, 32 had

clinically progressed and 26 were deceased at the time of study completion.

Progression-free survival

Peak height—An increase in the 90th percentile PH value between baseline and 1 month was a risk factor for PFS adjusted for the baseline heterogeneity (SD) of PH and the clinical control factors of baseline KPS, age, extent of resection, and gender (multivariate Cox regression, $P = .02$, hazard ratio [HR] = 5.408, 95% CI = 1.259–24.420). For every 1 unit increase in the change in the 90th percentile PH between baseline and 1 month (mean change = -0.02 ± 0.58), patients were at approximately a 5-fold greater risk for progression.

Percent recovery—Greater 25th percentile percent recovery at 2 months was a protective factor for PFS, adjusting for baseline KPS, age, extent of resection, and gender (multivariate Cox regression, $P = .009$, HR = 0.955, 95% CI = 0.926–0.987). For every 1% increase in percent recovery at 2 months (mean = 76.8% $\pm$ 14.7%), there was approximately a 5% reduction in the risk for progression. However, prior to this 2-month scan, the 25th percentile value of percent recovery at baseline and at 1 month was not found to be predictive of PFS (multivariate Cox regression adjusted for clinical control factors, $P = .46$ and .11, respectively). This supports the claim that by as early as 2 months into therapy, not only had differences in permeability emerged between response groups, but also the extent of permeability within the tumor region was further predictive of PFS.

Changes in parameters prior to progression

The data were also examined to identify changes in the perfusion parameters on the scans prior to patients' progression date that might be indicative of the imminent progression. Immediately prior to progression, there were no significant changes in the level of vascularization, in terms of both the 90th percentile value and the standard deviation (not shown). However, there were interesting changes in the percent recovery parameter prior to progression, which are displayed in Fig. 8. At 4 months prior to progression, the heterogeneity of recovery values within the putative tumor region began to increase (Fig. 8A, patient example Fig. 8E). There was a significant increase in the standard deviation of the recovery at 4 months prior to progression over the previous (6 months preprogression) scan (Fig. 8A, Wilcoxon sign-rank, $P < .04$). Patients with 12-month intermediate response were similar to the 6-month nonresponders at 4 months prior to progression in terms of both the 25th percentile recovery value and the overall standard deviation of recovery within the putative tumor region (Fig. 8B and C, Wilcoxon rank-sum, $P > .05$). Figure 8E shows the percent recovery parametric maps of a patient with a 12-month intermediate response leading up to progression. Note the increase in the heterogeneity of percent recovery within the putative tumor region at 4 months preprogression. This functional change can be seen on the percent recovery parametric map prior to the increase in enhancement on the T1-contrast-enhanced images (Fig. 8D). The observed changes in the percent recovery map are not limited to within the CEL (Fig. 8D), but rather are seen throughout the broader putative tumor region (Fig. 8E). Patients had very similar percent recovery levels at progression date (Fig. 8B and C, Wilcoxon rank-sum, $P > .2$). At progression, the mean percent recovery value was 76.2% $\pm$ 15.6%, and the mean standard deviation within the putative tumor region was 11.3% $\pm$ 5.4% for the entire population.

Overall survival

The greater 25th percentile percent recovery at 2 months into therapy was a protective factor for OS, adjusted for baseline KPS, age, extent of resection, and gender (multivariate Cox regression, $P = .02$, HR = 0.957, CI = 0.926–0.991). For each 1% increase in percent recovery at 2 months, there was an associated 4% reduction in the risk for death. Prior to the 2-month scan, percent recovery was not predictive of OS (multivariate Cox regression adjusted for clinical control factors, baseline $P = .08$ and at 1 month $P = .16$).

Discussion

DSC imaging was used to identify periods of vascular remodeling during the course of antiangiogenic therapy. Changes in the neovasculature that occurred within the first 2 months of therapy were related to both response and PFS. The marked decrease in PH that was observed during the first 2 months of therapy is consistent with the vascular normalization window that was reported by Batchelor et al.[3] They reported that the relative vessel size, as determined using a dual gradient- and spin-echo DSC sequence, reversed toward abnormal values at day 56 after initial therapy with AZD2171 and interpreted this as the end of the vascular normalization window.

When perfusion has normalized and the vasculature becomes more patent, it may be expected that intravascular gadolinium no longer leaks as readily into the extracellular extravascular space and that as a result the contrast enhancement on T1-weighted anatomical images decreases. This underlines the challenge in terms of using the standard response criteria to evaluate response to antiangiogenic therapy. The advantage of using 6- and 12-month assessments to analyze radiographic response to antiangiogenic therapy is that they incorporate the full pattern of response rather than just the date of progression. Some patients present with a marked decrease in contrast enhancement early in therapy that is suggestive of positive response, but possess a drastic return and/or growth of contrast enhancement by the 12-month assessment. Identifying which patients will have this pattern of response prior

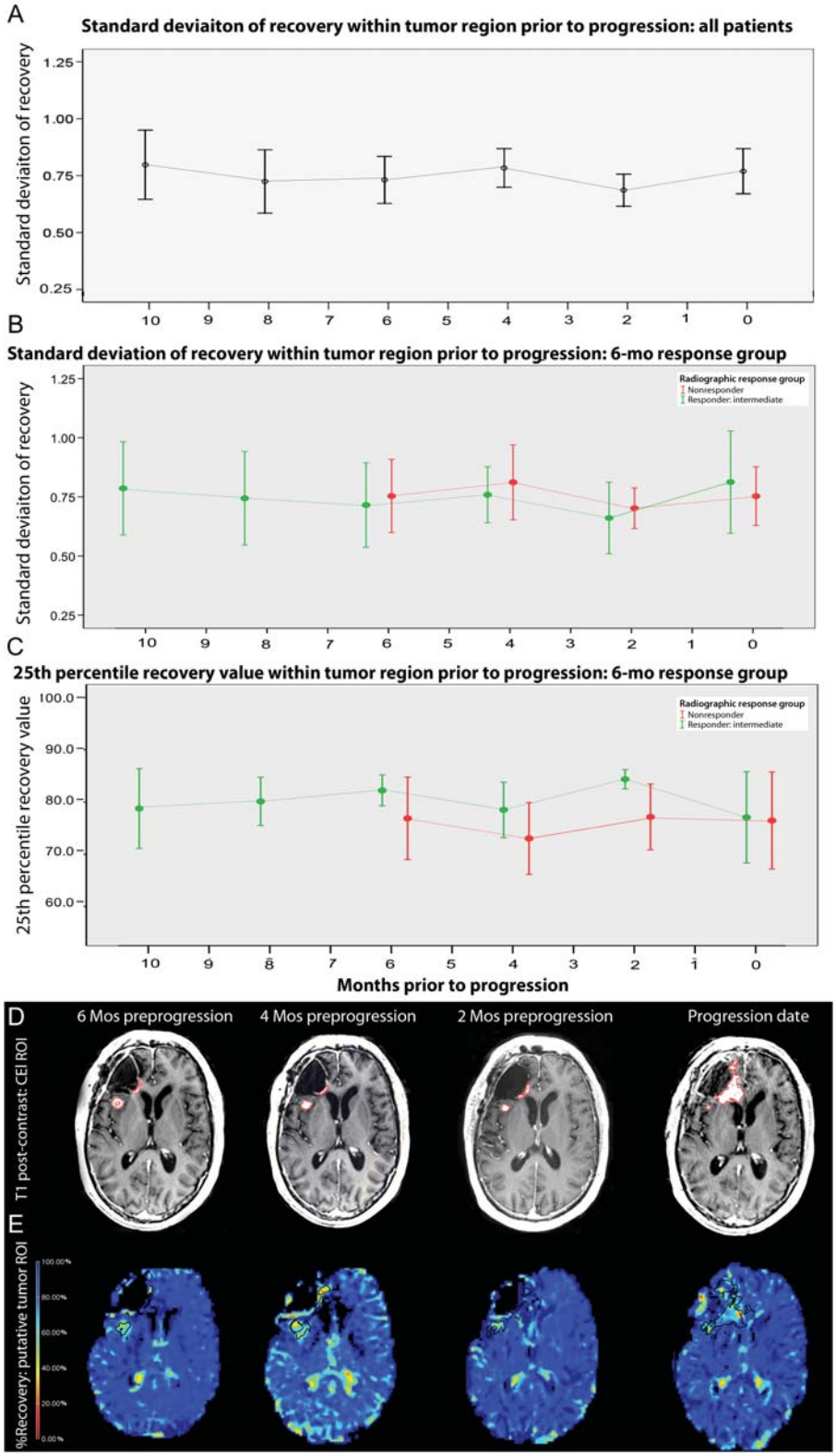

Fig. 8. Preprogression percent recovery. (A) Standard deviation of percent recovery within the putative tumor region increased 4 months prior to progression. (B and C) Both 6-month nonresponders and patients with a 12-month intermediate response converged as they neared progression in percent recovery intensity and heterogeneity. Note patient example showing an increase in heterogeneity of percent recovery (E) prior to the increase in CE (D).

to the resurgence of enhancement would allow alternative therapies to be considered at a time-point when they may be more effective. Interestingly, not all patients present in this way. Patients who show sustained response through both 6- and 12-month assessments may be interpreted as showing substantial benefit from antiangiogenic therapy. The ability to make an early distinction between these 2 patterns of radiographic response may therefore be of critical clinical importance for choosing the most effective therapy.

The disadvantage of using the 6- and 12-month response assessment is that it does not provide a continuous scale on which to measure response and to test predictive hypotheses. Although the use of the Macdonald criteria to evaluate PFS is limited in the evaluation of response to antiangiogenic therapy,[15] it does provide a scale for evaluating early biomarkers. OS may be a more appropriate endpoint in evaluating response to antiangiogenic therapy but is limited by the influence of salvage treatments.[15] The advantage in integrating the discrete 6- and 12-month radiographic assessment with the continuous PFS and OS scales is that 2 main challenges could be addressed: (i) elucidating perfusion differences in order to identify radiographic response groups and (ii) evaluating perfusion parameters during therapy that may predict outcome.

The subpopulation of patients who have a large decrease in vascular density after 1 month of therapy and an improvement in permeability after 2 months of therapy appeared to show the best response to therapy. Patients who show an increase in vascular density after 1 month of therapy and no improvement in permeability after 2 months did not respond within the first 6 months and thus had reduced PFS. In future prospective studies, this combination of early change in vascular density and permeability may be tracked as a biomarker of response and may ultimately aid in tailoring antiangiogenic therapy to individual patient characteristics.

The most challenging question lies in identifying patients who display an intermediate positive response to therapy but then suddenly progress. Patients with intermediate response showed a similar response pattern as patients with sustained response (decrease in vascular density after the first month and improvement in recovery after the second month) but had lower initial levels of vascularization. This suggests that an initially well-vascularized tumor, which improves in patency during initial therapy, is associated with better patient response. It seems that the combination of vascularization and permeability best describes the pattern of response.

Since most patients with GBM recur, it is critical to identify changes in perfusion that may be predictive of imminent progression.[17] When adjusted for the initial heterogeneity of tumor vascularization, the decrease in vascular density was predictive of PFS. This highlights interesting questions regarding the relationship between the extent and the spatial distribution of tumor vascularization and the PFS of patients on antiangiogenic therapy. The level of abnormal recovery that occurred after 2 months of therapy was predictive of both PFS and OS. Four months prior to progression, the heterogeneity of recovery within the putative tumor region began to increase, suggesting the end of the normalization period of the therapy for the individual patient and the beginning of reduced perfusion function. As Fig. 8D and E demonstrates, this change may occur prior to changes in appearance of the CEL, and it will be crucial to investigate the potential of this parameter in future studies.

The observation that the entire population, regardless of radiographic response group, had similar perfusion parameters at progression is suggestive of a "progression profile." In the radiographically challenging case of patients with 12-month intermediate response, perfusion parameters were similar to the 6-month nonresponders at 4 months prior to progression. However, these patients remained on therapy due to the stable appearance of their CEL. Early changes in the heterogeneity of percent recovery that may precede the increase in appearance of contrast enhancement have great potential for improving the management of patients on antiangiogenic therapy. Future prospective studies will validate these findings in a larger patient population and with other antiangiogenic therapies.

Conclusion

This study demonstrated changes in tumor vasculature on DSC MRI during the first 2 months of therapy for patients with GBM who were being treated with radiation therapy, temozolomide, and enzastaurin. Patients who had a large decrease in PH after 1 month of therapy and improvement in percent recovery after 2 months of therapy seemed to respond best, which may aid in identifying patients who would benefit most from antiangiogenic therapy in the future. The level of recovery present at the end of this 2-month normalization window was found to be predictive of PFS and OS. These results support the hypothesis that DSC perfusion imaging provides valuable information about changes in vascular function during therapy, which may ultimately aid clinicians in identifying patients who are likely to respond prior to therapy and as an early indicator of patient response to antiangiogenic therapy.

Acknowledgments

We gratefully thank Mary McPolin and Bert Jimenez of the Department of Radiology and Biomedical Imaging at UCSF for their assistance with data acquisition.

Conflict of interest statement. None declared.

Funding

UC Discovery grant (ITL-BIO04-10148); National Institute of Health (R01 CA127612, P01 CA11816); Joelle Syverson American Brain Tumor Association Fellowship.

References

1. Stupp R, Mason WP, van den Bent MJ, et al. Radiotherapy plus concomitant and adjuvant temozolomide for glioblastoma. *N Engl J Med*. 2005;352:987–996.
2. Stupp R, Hegi ME, Gilbert MR, Chakravarti A. Chemoradiotherapy in malignant glioma: standard of care and future directions. *J Clin Oncol*. 2007;25:4127–4136.
3. Batchelor TT, Sorensen AG, di Tomaso E, et al. AZD2171, a pan-VEGF receptor tyrosine kinase inhibitor, normalizes tumor vasculature and alleviates edema in glioblastoma patients. *Cancer Cell*. 2007;11:83–95.
4. Vredenburgh JJ, Desjardins A, Herndon JE, 2nd, et al. Phase II trial of bevacizumab and irinotecan in recurrent malignant glioma. *Clin Cancer Res.* 2007;13:1253–1259.
5. Friedman HS, Prados MD, Wen PY, et al. Bevacizumab alone and in combination with irinotecan in recurrent glioblastoma. *J Clin Oncol*. 2009;27:4733–4740.
6. Jain RK. Normalizing tumor vasculature with anti-angiogenic therapy: a new paradigm for combination therapy. *Nat Med*. 2001;7:987–989.
7. Jain RK, Tong RT, Munn LL. Effect of vascular normalization by antiangiogenic therapy on interstitial hypertension, peritumor edema, and lymphatic metastasis: insights from a mathematical model. *Cancer Res*. 2007;67:2729–2735.
8. Butowski N, Chang SM, Lamborn KR, et al. Enzastaurin plus temozolomide with radiation therapy in glioblastoma multiforme: a phase I study. *Neurooncology*. 2010;12:608–613.
9. Teicher BA, Alvarez E, Menon K, et al. Antiangiogenic effects of a protein kinase Cbeta-selective small molecule. *Cancer Chemother Pharmacol*. 2002;49:69–77.
10. Chen YB, LaCasce AS. Enzastaurin. *Expert Opin Investig Drugs*. 2008;17:939–944.
11. Tabatabai G, Frank B, Wick A, et al. Synergistic antiglioma activity of radiotherapy and enzastaurin. *Ann Neurol*. 2007;61:153–161.
12. Robertson MJ, Kahl BS, Vose JM, et al. Phase II study of enzastaurin, a protein kinase C beta inhibitor, in patients with relapsed or refractory diffuse large B-cell lymphoma. *J Clin Oncol*. 2007;25:1741–1746.
13. Wick W, Puduvalli VK, Chamberlain MC, et al. Phase III study of enzastaurin compared with lomustine in the treatment of recurrent intracranial glioblastoma. *J Clin Oncol*. 2010;28:1168–1174.
14. Butowski NALK, Chang S,, Hsieh E, et al. Phase II and pharmacogenomics study of enzastaurin plus temozolomide and radiation therapy in patients with glioblastoma multiforme or gliosarcoma.Paper presented at: Proceedings of 2009 American Society of Clinical Oncology Annual Meeting, Abstract No. 2020. San Francisco, CA: University of California–San Francisco; Indianapolis, IN: Eli Lilly. 2009.
15. van den Bent MJ, Vogelbaum MA, Wen PY, Macdonald DR, Chang SM. End point assessment in gliomas: novel treatments limit usefulness of classical Macdonald's Criteria. *J Clin Oncol*. 2009;27:2905–2908.
16. Macdonald DR, Cascino TL, Schold SC, Jr, Cairncross JG. Response criteria for phase II studies of supratentorial malignant glioma. *J Clin Oncol*. 1990;8:1277–1280.
17. Chang SM, Lamborn KR, Kuhn JG, et al. Neurooncology clinical trial design for targeted therapies: lessons learned from the North American Brain Tumor Consortium. *Neurooncology*. 2008;10:631–642.
18. Wong ET, Brem S. Taming glioblastoma: targeting angiogenesis. *J Clin Oncol*. 2007;25:4705–4706.
19. Fukumura D, Jain RK. Imaging angiogenesis and the microenvironment. *APMIS*. 2008;116:695–715.
20. Harrer JU, Hornen S, Oertel MF, Stracke CP, Klotzsch C. Comparison of perfusion harmonic imaging and perfusion MR imaging for the assessment of microvascular characteristics in brain tumors. *Ultraschall Med*. 2008;29:45–52.
21. Saraswathy S, Crawford FW, Lamborn KR, et al. Evaluation of MR markers that predict survival in patients with newly diagnosed GBM prior to adjuvant therapy. *J Neurooncol*. 2009;91:69–81.
22. Law M, Yang S, Wang H, et al. Glioma grading: sensitivity, specificity, and predictive values of perfusion MR imaging and proton MR spectroscopic imaging compared with conventional MR imaging. *AJNR Am J Neuroradiol*. 2003;24:1989–1998.
23. Sorensen AG, Batchelor TT, Zhang WT, et al. A "vascular normalization index" as potential mechanistic biomarker to predict survival after a single dose of cediranib in recurrent glioblastoma patients. *Cancer Res*. 2009;69:5296–5300.
24. Park I, Chen AP, Zierhut ML, Ozturk-Isik E, Vigneron DB, Nelson SJ. Implementation of 3 T lactate-edited 3D (1)H MR spectroscopic imaging with flyback echo-planar readout for gliomas patients. *Ann Biomed Eng*. Published online ahead of print July 23, 2010.
25. Nelson SJ, Nalbandian AB, Proctor E, Vigneron DB. Registration of images from sequential MR studies of the brain. *J Magn Reson Imaging*. 1994;4:877–883.
26. Lupo JM, Cha S, Chang SM, Nelson SJ. Dynamic susceptibility-weighted perfusion imaging of high-grade gliomas: characterization of spatial heterogeneity. *AJNR Am J Neuroradiol*. 2005;26:1446–1454.
27. Rueckert D, Sonoda LI, Hayes C, Hill DL, Leach MO, Hawkes DJ. Nonrigid registration using free-form deformations: application to breast MR images. *IEEE Trans Med Imaging*. 1999;18:712–721.
28. Zhang Y, Brady M, Smith S. Segmentation of brain MR images through a hidden Markov random field model and the expectation-maximization algorithm. *IEEE Trans Med Imaging*. 2001;20:45–57.
29. Saraswathy SCF, Nelson S.J. Semi-automated segmentation of brain tumor lesions in MR images. Paper presented at: Proceedings of the 14th Annual Meeting of International Society of Magnetic Resonance in Medicine, Seatle, WA, Abstract No. 1609. 2006.
30. McKnight TR, von dem Bussche MH, Vigneron DB, et al. Histopathological validation of a three-dimensional magnetic resonance spectroscopy index as a predictor of tumor presence. *J Neurosurg*. 2002;97:794–802.
31. Wen PY, Macdonald DR, Reardon DA, et al. Updated response assessment criteria for high-grade gliomas: response assessment in neuro-oncology working group. *J Clin Oncol*. 2010;28:1963–1972.